Journal of the Korean Nuclear Society
Volume 34, Number 1, pp.68~79, February, 2002

A Heuristic Application of Critical Power Ratio to Pressurized Water Reactor Core Design

Seung-Hoon Ahn
Korea Institute of Nuclear Safety
19 Gusong-dong, Yusong-gu, Taejon, 305-600, Korea
k175ash@kins.re.kr
Gyoo-Dong Jeun
Hanyang University
17 Haengdang-dong, Sungdong-gu, Seoul, 133-791, Korea

(Received October 15, 2001)

Abstract

The approach for evaluating the critical heat flux (CHF) margin using the departure from nucleate boiling ratio (DNBR) concept has been widely applied to PWR core design, while DNBR in this approach does not indicate appropriately the CHF margin in terms of the attainable power margin-to-CHF against a reactor core condition. The CHF power margin must be calculated by increasing power until the minimum DNBR reaches a DNBR limit. The Critical Power Ratio (CPR), defined as the ratio of the predicted CHF power to the operating power, is considered more reasonable for indicating the CHF margin and can be calculated by a CPR correlation based on the heat balance of a test bundle. This approach yields directly the CHF power margin, but the calculated CPR must be corrected to compensate for many local effects of the actual core, which are not considered in the CHF test and analysis. In this paper, correction of the calculated CPR is made so that it may become equal to the DNB overpower margin. Exemplary calculations showed that the correction tends to be increased as power distribution is more distorted, but are not unduly large.

Key Words : CHF, DNBR, CPR, PWR, local flow condition, heat balance

1. Introduction

Traditionally the CHF margin, for low quality region representative of PWR operating conditions, has been expressed in terms of the Departure from Nucleate Boiling Ratio (DNBR) defined as the ratio of the predicted CHF to the actual local heat flux. In this approach, the CHF is usually predicted by the empirical correlation where the CHF is an explicit function of local flow conditions. Normally the DNBR margin is evaluated by comparing the minimum DNBR calculated against various operating conditions with a DNBR limit covering the uncertainty of the

correlation against the experimental data.

As pointed out by several researchers [1,2], the DNBR margin may significantly differ from the power margin-to-CHF and the numerical value of the DNBR depends on the CHF correlation used. In this viewpoint, DNBR itself is not appropriate for providing the real CHF margin of a reactor core condition in terms of how far away from a CHF condition the current operating condition is. The Critical Power Ratio (CPR), defined as the ratio of the predicted CHF power to the operating power, is considered more meaningful, because it provides an estimation of the real CHF margin in terms of the freedom to overshoot the current reactor power.

There are two approaches for calculating the CPR: one is to use a DNBR correlation with successive increase of power until the CHF condition is reached, and the other is to use a CPR correlation which directly includes the heat balance as part of the correlation. The first approach is more general in the Pressurized Water Reactor (PWR) community since it can handle cross-flow and thermal mixing in open multiple channels, while requiring an iterative calculation of the CHF power against DNBR. In the latter approach, the calculated CPR against a reactor core condition indicates directly the available power margin-to-CHF, however, it is argued that this approach cannot handle many realistic situations of a reactor core, e.g., fast transients, complex heat flux profiles which vary axially and radially, hot spots in various heat flux shapes, and cross flow and thermal mixing between channels [3]. It is true in that the CPR correlation, based on the heat balance of a particular test condition, does not reflect many possible local effects at the actual reactor core. Nevertheless, use of the CPR correlation approach could be allowed in the engineering field only if the calculated CPR is not significantly deviated from that by the DNBR approach at any anticipated operating conditions of conventional reactor designs and is adjusted by appropriate correction factors.

In this paper, the two approaches by DNBR and CPR correlations are assessed by (a) constructing correlations against the selected CHF data and (b) evaluating the power margins-to-CHF against the actual core configuration. The mixing between channels due to three dimensional power distribution at the actual core is considered as one of conditions at which applicability of the CPR correlation approach to PWR core design may be intimated.

2. Approaches for Evaluating CHF Margin

2.1. Traditional DNBR Approach

The background of the approaches for evaluating the CHF margin is recalled by introducing the traditional DNBR approach as seen in Fig. 1. In this approach the CHF margin is defined as the distance from the local heat flux to the CHF at the same location:

$$\delta q'' / q_c'' = 1 - (q_{loc}'' / q_c'') . \quad (1)$$

This expression is based on the local condition hypothesis which has been verified by several researchers, although it is recognized that the CHF is somewhat affected by the upstream conditions [4,5,6]. If the CHF tests are performed with the model geometry to well describe thermal hydraulic behavior in any hot region of the actual reactor core, extrapolation of the test results to the in-reactor condition is made possible by applying the empirical correlation directly to local flow conditions. In other words, it is assumed that at the same local flow condition, the measured CHF at a test bundle, q''_m is equal to the CHF at the actual core, q''_c.

In general, the mean conditions at the test bundle and at the actual core, e.g., inlet temperature, average mass flux, exit pressure, are known, while a specific tool is needed to obtain the local flow conditions. In order to obtain local flow conditions which are usually determined at the scale of a subchannel surrounded by 3 or 4 rods, a procedure described as "subchannel analysis" is generally used with the help of a computer code implementing the procedure (A and A' of Fig.1) [7]. Using the ratio of the measured-to-predicted CHFs by a DNBR correlation, and the definition of DNBR, the CHF margin of Eq.(1) is expressed by DNBR:

$$DNBRM = 1 - \frac{1}{R_1}\frac{1}{DNBR} \quad (2)$$

The accuracy of a correlation for a particular fuel design is determined by evaluating the statistics of R_1 in terms of the mean and the standard deviation. Then the correlation is used to calculate the minimum DNBR at various core mean conditions by the same subchannel analysis code which has been used for correlation development (B of Fig.1). Because the CHF margin is required to be greater than and equal to zero with sufficient confidence level during normal operation and anticipated transients, the minimum DNBR (MDNBR) in Eq.(2) is,

$$MDNBR \geq \frac{1}{|R_1|_{95/95\,LTL}} \quad (3)$$

where a subscript, 95/95LTL means the lower tolerance limit determined at 95 % probability and 95 % confidence levels, then the reciprocal of the 95/95LTL of R_1 is often called as a DNBR correlation limit (LDNBR) [8]. The conventional design process is to confirm that there is a sufficient margin to compensate for DNBR degradation from the current operating condition

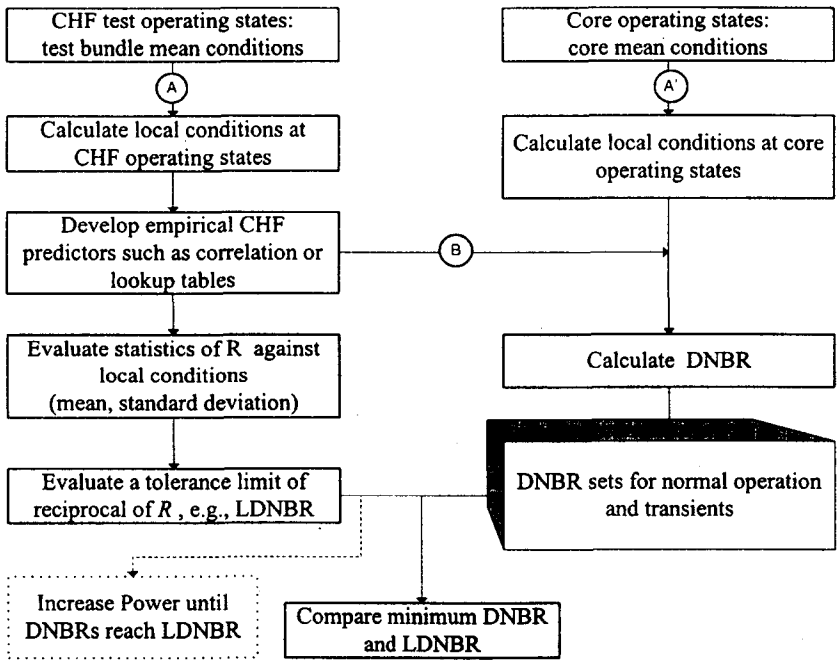

Fig. 1. Traditional DNBR Approach for Evaluating CHF Margin in a PWR

to any anticipated transients by demonstrating that Eq. (3) is met for all anticipated operating conditions. In addition the plant design installed with the upgraded system for core monitoring and protection requires the DNBR to be converted to DNB-OverPower Margin (DNB-OPM) of the meaning similar to CPR, which is used to determine the input constants of the system software, accompanying supplementary analyses as seen inside the dotted line of Fig. 1. The DNB-OPM is calculated by increasing power until MDNBR reaches LDNBR.

2.2. CPR Correlation Approach

The simplest way to avoid the complexity in DNBR approach where the CHF power must be searched by iterating power against DNBR is to express the CHF margin by the critical power instead of the critical heat flux in Eq.(1):

$$\delta PO / PO_c = 1 - (PO_a / PO_c). \tag{4}$$

Using the critical power measured at a test bundle, PO_m, Eq. (4) is rearranged:

$$\delta PO / PO_c = 1 - \frac{1}{\varphi} \frac{1}{R_2} \frac{1}{CPR}, \tag{5}$$

where $\varphi = PO_c/PO_m$ and $R_2 = PO_m/PO_p$.

For a round tube coolant channel where heat balance holds, the terms by power in Eq.(5) can be directly converted to the terms by local heat flux, assuming that axial heat flux distribution does not change with power. If a round tube correlation is constructed by considering heat balance from channel inlet to the CHF location, then the minimum CPR becomes equal to the ratio of the predicted CHF to the local heat flux at the limiting location. In this case, φ is equal to unity and the CPR margin in Eq.(5) becomes

$$CPRM = 1 - \frac{1}{R_2} \frac{1}{MCPR}, \tag{6}$$

where the accuracy of the CPR correlation is determined by evaluating statistics of R_2. The reciprocal of the 95/95LTL of R_2 represents for the tolerance limit of the CPR correlation in the same way as in the DNBR approach, and is termed as a CPR correlation limit (LCPR).

However, Eq.(6) is not directly applicable for the actual core which is composed of the large number of coolant channels, because there exists interchange of mass and energy between the subchannels and heat balance does not hold for the coolant channel of interest. Even for a CHF test at the assembly of rod arrays, heat retained in the channel of interest is not always same as heat generated in the channel. As attempted by some researchers [1,10], it is possible to construct a CPR correlation so that system parameter concept of assembly power can be interchanged to local condition concept of local heat flux. However, it is questionable whether the CPR correlation based on a test bundle condition is still valid for the different cases of mass and enthalpy distribution, for example, such as extended test bundle size and different power distribution.

Recognizing such limitations of the CPR correlation, it is asked as to how far CPR calculated by a CPR correlation is deviated from the CHF power calculated by the DNBR approach. The basic idea is to correct the CPR in Eq.(5) by φ. In DNBR approach, DNB-OPM is indicates the power margin available until MDNBR reaches LDNBR determined at a 95/95 probability and confidence level, then,

$$DNBOPM = \left| \frac{PO_c}{PO_a} \right|_{95/95LTL} = \varphi \times MCPR \times |R_2|_{95/95LTL} \tag{7}$$

Therefore, a correction factor, φ is defined by

$$\varphi = \frac{DNBOPM_{DNBR=LDNBR}}{MCPR/LCPR},$$

and the corrected CPR is

$$MCPR_{corrected} = \varphi \times MCPR \quad (9)$$

In particular, attention must be paid to the definition of each parameter; DNB-OPM and CPR are in direction of the margins from the current to critical conditions while DNBRM and CPRM, in the opposite direction. In addition, the uncertainty of the CPR correlation is not involved in the corrected MCPR unlike DNB-OPM, therefore, MCPR must be divided by LCPR whenever DNB-OPM and MCPR are compared each other, Applicability of a CPR correlation approach to a PWR core thermal design lies on whether the correction factor can be obtained on generic basis. It seems to be feasible for the current reactor design whose anticipated core operating conditions are well known. If the values of the correction factor φ are determined against various operating conditions, a safety requirement for the CHF margin is satisfied by demonstrating that the corrected MCPR, $MCPR_{corrected}$ is greater than or equal to LCPR:

$$MCPR_{corrected} \geq LCPR \quad (10)$$

3. Application of DNBR and CPR Correlations

3.1. Correlation Types and Forms

The correlations types are classified into those (a) basically based on local flow conditions at the location of interest and (b) incorporating heat balance along the channel up to the point of interest into local flow conditions at the same point. The first type of correlations typically has the form:

$$q''_{p,1} = \frac{A - x}{C}, \quad (11)$$

where A and C are the unspecified functions of G_{loc}, P, and D_e. The CHF margin is expressed in terms of DNBR in applying this type of correlations to a reactor core condition.

The second type of correlations is obtained by looking for intersection of the heat balance curve and the CHF curve of Eq. (11), then, the well-known EPRI generalized correlation [11] is obtained:

$$q''_{p,2} = \frac{A' - x_{in}}{C' + \frac{x - x_{in}}{q''}} \quad (12)$$

where A' and C' are also the unspecified functions of G_{loc}, P, and D_e. This type of correlations yields CPR by the ratio of the predicted CHF to the local heat flux, assuming that axial heat flux distribution does not change with power.

3.2. Construction of Correlations

The DNBR and the CPR correlations were constructed for the CHF data used for CE-1 correlation development [11]. Data are available from those compiled at Heat Transfer Test Facility (HTRF) of Columbia University [12], e.g., data in test sections 21.0, 36.1, 38.0, 47.0, 48.0, and 52.0. The correlations of Eqs.(11) and (12), using the functional forms of A, A', C and C' proposed by Macbeth [13], fitted with the CHF data by a regression analysis [14].

Because statistical F and t-tests [15] for subsets of the CHF data with different heated lengths indicated that there is a statistical dependence between them, a parameter, heated length was additionally included in the power function of G in the predetermined functional forms; that is,

Table 1. Optimized Coefficients of DNBR and CPR Correlations and Regression Ranges

Coefficients	Values	
	DNBR Correlation	CPR Correlation
a1	0.55894	0.48713
a2	-0.53001	-0.59349
a3	2.263×10^{-4}	1.862×10^{-4}
a4	0.59889	0.54729
a5	-0.81900	-0.78120
a6	-0.45094	-0.35381
a7	0.32486	0.43832
a8	-0.30446	-0.15107
a9	0.09321	0.04363
a10	0.16272	0.07516
Regression range for each parameter		
Pressure	9.6 to 16.7	MPa,
Local mass flux	1.22×10^{3} to 5.42×10^{3}	kg/m^2 sec
Local quality	-0.1 to 0.2	
Heated length	2.13 to 3.81 m	

$$A, A' = a_1 \tilde{P}^{a_2} \tilde{G}_{loc}^{\,a_5+a_7\tilde{P}+a_9 L} \tag{13}$$

$$C, C' = a_3 \tilde{P}^{a_4} \tilde{G}_{loc}^{\,a_6+a_8\tilde{P}+a_{10} L} \tag{14}$$

where $\tilde{P} = P/10$ and $\tilde{G}_{loc} = G_{loc}/10^2$ and a_1, a_2, ··· a_{10} are the correlation coefficients which are obtained by a regression analysis.

A thermal hydraulic subchannel analysis code, COBRA-IV-i [16] was used to obtain the local flow condition at the measured CHF site. The major input options chosen of the computer code are: Levy model for subcooled void, modified Armand correlation for bulk void fraction, Armand correlation for two-phase friction multiplier, and use of thermal diffusion coefficient of 0.02 for turbulent mixing, etc.

The coefficients of each correlation were optimized so as that the mean of the ratio of the measured and predicted CHF, $X(R)$ approaches unity over the regression range. Table 1 summarizes the optimized coefficients and the regression ranges. The predicted CHFs against the measured CHFs, when using the DNBR and CPR correlations, are presented in Figs. 2 and 3 respectively.

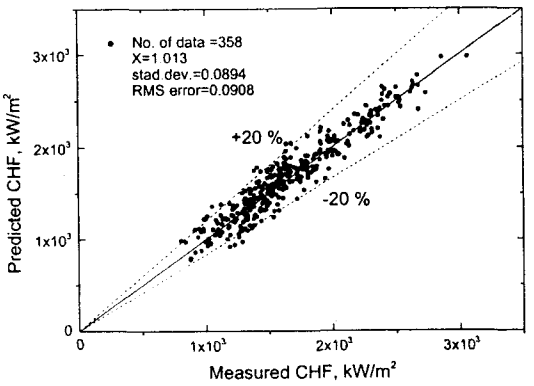

Fig. 2. Predicted CHF Against Measured CHF by DNBR Correlation

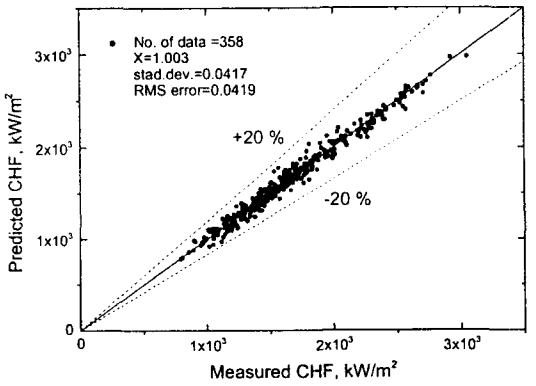

Fig. 3. Predicted CHF Against Measured CHF by CPR Correlation

In these figures, the statistical parameters, *STD* and *RMS* are defined:

$$\mathrm{STD} = \sqrt{\frac{1}{N-1}\sum_{i=1}^{N}(R - X(R))^2} \tag{15}$$

$$\mathrm{RMS} = \sqrt{\frac{1}{N}\sum_{i=1}^{N}(R-1)^2} \tag{16}$$

Then, the limit of each correlation is determined

by:

$$\text{LDNBR or LCPR} = \frac{1}{X(R) - k_{95/95}STD}, \quad (17)$$

where $k_{95/95}$ is given by Owen's tables [17] such that at least 95 percent of the population of R is greater than $X(R) - k_{95/96}STD$ with confidence of 0.95. When this method was carried out using all 358 data points, LDNBR and LCPR were 1.17 and 1.08 respectively.

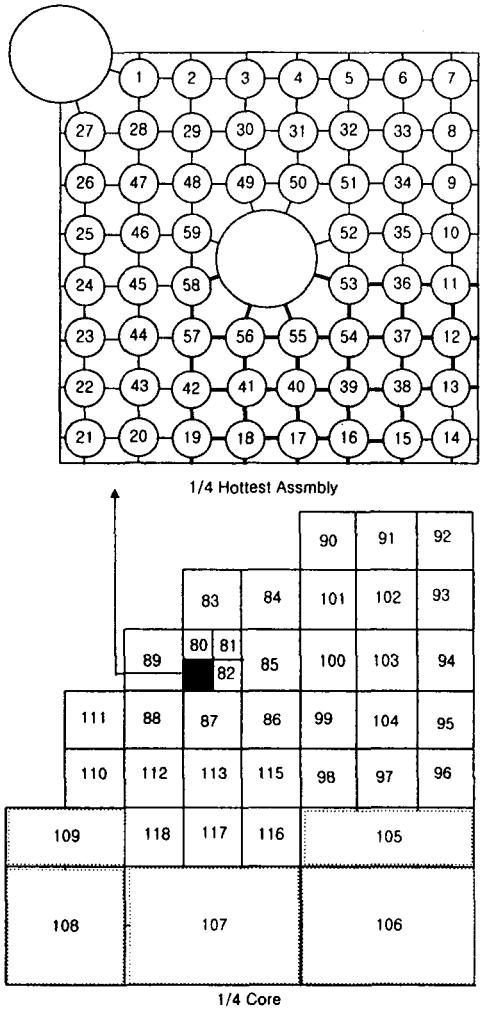

Fig. 4. Three-Dimensional Modeling of a Reactor Core for Subchannel Analysis

3.3. Exemplary Analyses

3.3.1. Case Selection

In order to assess the two approaches for evaluating the CHF margin at a PWR core operating conditions, exemplary calculations were performed for the following two cases:

(a) A normal operating condition at 100 percent power and

(b) A state point condition with distorted axial and radial power distribution as a result of uncontrolled withdrawal of the control element assemblies at 10 percent power.

Data are available from sections 4.4 and 15.4 of the final safety analysis report of Yonggwang units 3 and 4 nuclear power plants [18]. Figure 4 shows a detailed subchannel modeling of the selected reactor core, assuming quadrant symmetry of radial power distribution. In this figure, the regions surrounded by the solid line are the candidates where DNBR is expected to be the lowest.

Table 2 shows the values of the major operating parameters considered for analysis. In this table, the axial shape index, ASI is defined by difference

Table 2. Values of Parameters Considered for Analysis

Parameter	Case (a)	Case (b)
Core average heat flux, kW/m^2	567.04	238.16
Core top pressure, MPa	15.51	14.48
Average core mass flux, kg/m^{2}sec	356.69	338.83
Core inlet temperature, ℃	295.83	300.
Hottest rod F_r	1.550	3.970
Hottest assembly F_r	1.325	3.394
Axial power distribution	1.26 peak ASI = -0.070	1.58 peak ASI = -0.300

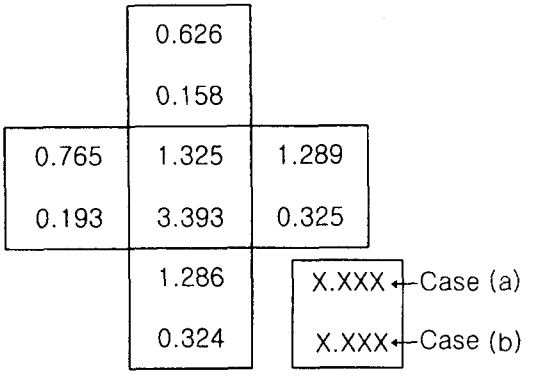

Fig. 5. Radial Peaking Factors of Hottest Assembly and Its Assembly

between powers in the upper half and the lower half of the core divided by the total core power. The values of the parameters for case (b) were selected at the time that the MDNBR is the lowest during the transient, with assumption of radial power peaking factors of the hottest assembly and its adjacent assemblies as seen Fig.5. In this figure, the average power of the assemblies surrounding the hottest assembly is decreased by increased power of the hottest assembly, while other assemblies maintain the radial peaking factors of case (a). This assumption maximizes mass and enthalpy interchange between the hot assembly and its adjacent assemblies.

3.3.2. Determination of Correction Factor

In order to apply the two CHF correlations of Eqs.(11) and (12) to the selected cases, the factors which compensate for the effects of cold wall and non-uniform axial heat flux distribution must be included in the correlations. Then the DNBR correlation has the form:

$$q''_{p,1} = \frac{F_{cw}}{F}\frac{A-x}{C} \tag{19}$$

Also considering the relationship of Eqs.(11) and (12), the CPR correlation is

$$q''_{p,2} = \frac{F_{cw}(A'-x_{in})}{FC' + F_{cw}\dfrac{x-x_{in}}{q''}} \tag{20}$$

Table 3. Comparison of Calculated MDNBR and MCPR

Case	MDNBR	MCPR	MDNBR (CE-1)
(a)	1.942 (347.0 cm)	1.415 (347.0 cm)	2.028 (347.0 cm)
(b)	2.334 (342.9 cm)	1.750 (342.9 cm)	2.513 (342.9 cm)

*Values in parentheses mean the distance from inlet to MDNBR or MCPR locations

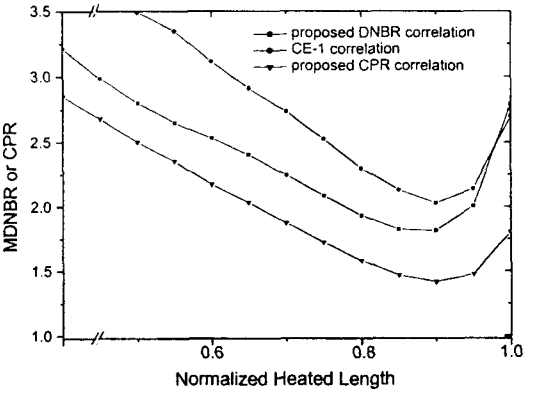

Fig. 6. DNBR and CPR in Each Axial Position of Hottest Rod of Case (a)

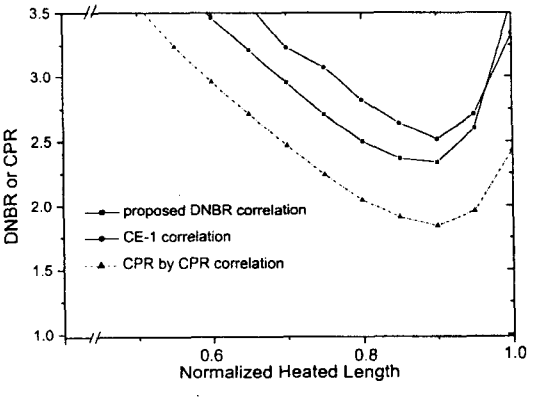

Fig. 7. DNBR and CPR in Each Axial Position of Hottest Rod of Case (b)

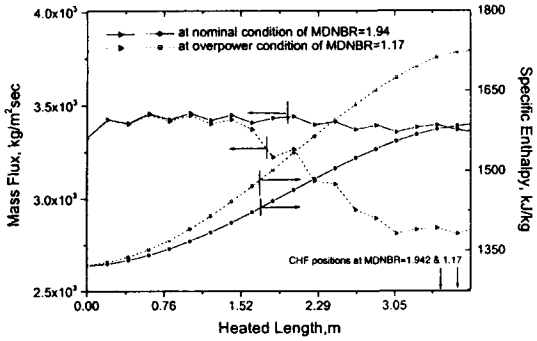

Fig. 9. Variation of Mass and Enthalpy along Hottest Channel of Case (a)

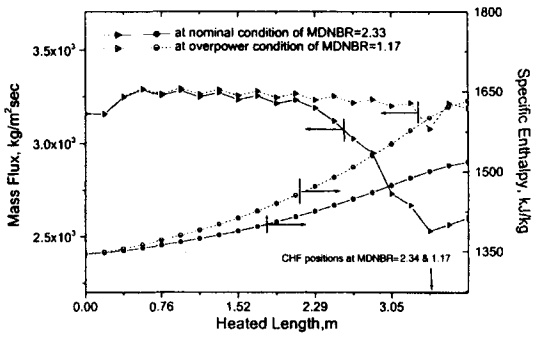

Fig. 10. Variation of Mass and Enthalpy along Hottest Channel of Case (b)

For simplicity, the cold wall factor of the CE-1 correlation [11] and Tong' s non-uniform factor [6] were used for F_{cw} and F respectively.

The calculated result for above two cases is presented in Table 3, showing that the numerical value of MCPR is lower than that of MDNBR. Three correlations all, including CE-1 correlation, yield MDNBR or MCPR at the rod of No.54 and its adjacent guide tube subchannel in Fig.4. The DNBR and CPR values at each axial position of the no.54 rod for cases (a) and (b) are plotted in Figs.6 and 7 respectively. The CPR correlation has more smooth shape, when compared with DNBR correlations.

The DNB-OPM was also calculated for each case by increasing the power until MDNBR reaches LDNBR determined by Eq.(17). The MDNBR positions for normal and overpower conditions of case (a) were not the same, though the difference of MDNBR itself was very small, e.g., 0.02. As shown in Figures 8 and 9, variations of mass flux and enthalpy along the hottest subchannels become larger due to increase of mass flow out from hot region as power increases. For each case, correction of the calculated CPR was made by using Eq.(8). Table 4 shows the values of φ for two cases. Comparison of the two implies that the calculated CPR goes farther from the DNB-OPM, as distortion of power distribution becomes more significant. However, considering that extremely distorted power distribution during CEA withdrawal transient at low power was used for analysis, it is expected that the value of φ will not be unduly increased for other transients with power distribution anomaly.

3.3.3. Discussions

3.3.3.1. Accuracy of Correlation

Some attempts [1,19,20] have been made to

Table 4. Correction Factors for Normal and Distorted Power Distributions

Cases	CHF Margin against DNBR and CPR Correlation Limits				
	DNBR Margin by Eq.(3)	CPR Margin by Eq.(6)	DNB-OPM to LDNBR ①	$\frac{\text{MCPR}}{\text{LCPR}}$ ②	φ = ① / ②
(a)	39.7 % DNBR	23.7 %	126.9 %	1.311	0.968
(b)	49.8 % DNBR	41.3 %	145.5 %	1.620	0.898

compare the accuracies of different correlations of predicting the CHF data published by EPRI [10]. When statistics of the ratio of the predicted-to-measured CHF were determined against correlations of consideration and were compared, they concluded that the EPRI correlation [12] has the best accuracy of all correlations compared. Such approach is inappropriate and can be misleading as pointed out by several researchers [3,21], while a data correlating process explains the reason why the correlarions, yielding the CPR statistics as the EPRI correlation does, have better accuracy than the correlations, yielding the DNBR statistics.

If the CHF data are predicted by a CPR correlation, the relation of the i-th measured CHF and the predicted CHF is:

$$q''_{m,i} = q''_{p,2} + \varepsilon_{i,2} \tag{21}$$

where i is the test run number, and ε, the i-th residual error. Eq.(17) can be rewritten by using Eqs.(10) and (11):

$$q''_{m,i} = q''_{p,1} + \varepsilon_{i,2}\left(1 + (\chi - \chi_{in}) / Cq''_{m,i}\right). \tag{22}$$

The total residual error by a DNBR correlation against the CHF data become always larger than that by a CPR correlation, neglecting the second order term:

$$\sum_i \varepsilon_i^2\Big|_1 = \sum_i \varepsilon_i^2\Big|_2 + \sum_i \varepsilon_i^2\Big|_2 \left(\frac{2(\chi - \chi_{in})_i}{Cq''_{m,i}}\right). \tag{23}$$

Inclusion of heat balance parameter $(\chi - \chi_{in})/q''$ makes the residual error of the CPR correlation smaller than that of the DNBR correlation. It is due to the fact that the CHF is a decreasing function of local quality; inversely, if the CHF is a increasing function of local quality, the CPR error would be larger than the DNBR error by the last term of eq.(19).

3.3.3.2. Intrinsic Problems of CPR Correlation

Regardless of the better accuracy of the CPR correlation, the CPR correlation has the two intrinsic problems when applying to PWR rod bundles: One is that for steady state and quasi-steady conditions the effect of 3-dimensional mass and enthalpy distribution in a reactor core is neglected in a CPR correlation, and the other is that this approach does not reflect the upstream condition changed as power increases, for example, such as change of MDNBR location. As a result, the CPR correlation approach yields the CHF power margin different from that by the DNBR approach. Therefore, correction of the calculated CPR must be made so that the CPR and DNB-OPM may be compared at their respective correlation limits.

Corrections of the calculated CPR were for the cases where MDNBR location is almost unchanged as power increases. Actually there exists the condition where the MDNBR location moves from one subchannel to the other. In order to examine the case where the MDNBR location is moved from guide thimble to typical cells, the condition of case (a) was arbitrarily manipulated, so that MDNBR location may vary as power. Radial peaking factor of 1.80 was assigned for the rods of no.16, 17, 39 and 40, instead of their original values 1.550, 1.550, 1.532, and 1.532, as other conditions are held fixed. At this condition

Table 5. Effect of MDNBR Location on Correction Factor

MDNBR at nominal power (rod no./distance)	MDNBR at overpower (rod no./distance)	DNB -OPM to LDNBR	MCPR / LCPR	φ
1.800 (54/347cm)	1.171 (40/367.8cm)	115.8 %	1.226	0.940

the MDNBR value 1.800 was obtained at the location of rod no.54. When increasing the power until MDNBR reaches LDNBR, the MDNBR location was moved to rod no.40. Table 5 shows that the calculated value of φ does not largely changed from that for case (a). From this example, the correction factor appears not to be significantly affected by the change of the MDNBR location.

4. Conclusions

In this paper two approaches by DNBR and CPR correlations were assessed by constructing correlations against the selected CHF data and by evaluating the power margins-to-CHF against two power distributions in the actual core condition. The following conclusions are drawn from this study:

(a) The relatively higher prediction accuracy of the CPR correlation, compared with the DNBR correlation, is attributed to a CHF characteristic, which is a decreasing function of local quality.

(b) The calculated CPR goes farther from the DNB-OPM, as power distribution is more distorted, however, the required correction of CPR is not unduly large even for CEA withdrawal at low power under consideration.

(c) Further examination for various power distributions is needed, in order to determine the range of correction of CPR covering any anticipated operating conditions.

Nomenclature

D_e	hydraulic equivalent diameter (cm)
F	Tong' s non-uniform factor
F_{cw}	cold wall factor
G	mass velocity (kg/m2 · sec)
P	system pressure (MPa)
PO	test bundle power or core power (kW)
q''	heat flux (kW/m^2)
R	ratio of measured and predicted CHF
RMS	root-mean-square error
STD	standard deviation
$X(R)$	mean of R

Greek symbols

ε	residual error
χ	thermodynamic quality

Subscripts

a	actual
c	critical heat flux condition
in	inlet condition
m	measured value of CHF or critical power
p	predicted value of CHF or critical power
loc	local condition

References

1. G.S. Lellouche, "The Boiling Transition: Analysis and Data Comparisons," *Nucl. Engrg. & Des.* **116**, 117-133 (1989).
2. Pavel Hejzlar and Neil E. Todreas, "Consideration of CHF Margin Prediction by Subcooled or Low-Quality CHF Correlations," *Nucl. Engrg. & Des.* **163**, 215-223 (1996).
3. Moshe Siman-Tov, "Application of Energy Balance and Direct Substitution Methods for Thermal Margins and Data Evaluation," *Nucl. Engrg. & Des.* **163**, 249-258 (1996).
4. R. Ayed and J.P. Bourteele, "Theoretical Evaluation of Currently Used Critical Heat Flux Correlations," *Trans. ANS*, Vol. 59, Atlanta June (1989).
5. R.V. Macbeth, "An Appraisal of Forced Convection Burnout Data," *Proc. Instn. Mech. Engrs.* **Vol.180 Pt 3C** (1965-1966).
6. L.S. Tong, "Boiling Crisis and Critical Heat Flux," U.S. AEC. TID-25887 (1972).

7. J. Weisman, "Methods for Detailed Thermal and Hydraulic Analysis of Water-Cooled Reactors," *Nucl. Sci. & Engrg.*, **57**, 255-276 (1975).
8. F.de.Crecy, "A New Approach to the MDNBR Concept," *Nucl. Engrg. & Des.* **149**, 243-249 (1994).
9. C.R. Lehmann, "Transient Thermal-Hydraulic Analysis: Impact on Technical Specifications," Combustion Engineering Inc. TIS-6826.
10. D.G. Reddy and C.F. Fighetti, "Parametric Study Of CHF Data Vol.2: A Generalized Subchannel CHF Correlation for PWR and BWR Fuel Assemblies," EPRI-NP-2609, (1982).
11. F.D. Lawrence et al., "Critical Heat Flux in PWR Fuel Assemblies," *AIChE-ASME Heat Transfer Conf.*, Salk Lake City, Utah, Aug. 15-17 (1977).
12. D.G. Reddy and C.F. Fighetti, "Parametric Study of CHF Data Vol.3: Critical Heat Flux Data," EPRI-NP-2609 (1982).
13. R.V. Macbeth, "Burnout Analysis, Part 4: Application of a Local Condition Hypothesis to World Data for Uniformly Heated Round Tubes and Rectangular Channels," U.K. AEA report, AEEW-R267 (1963).
14. SAS User' s Guide: Statistics, Version 5 Edition, SAS Institution Inc. (1985).
15. L.C. Edwin et al., "Statistics Manual, Dover Publications Inc., New York (1956).
16. C.L. Wheeler et al., COBRA-IV-i: An Interim Version of COBRA for Thermal Hydraulic Analysis of Rod Bundle Nuclear Fuel Elements and Cores, BNWL-1962, (1976).
17. D.B. Owen, "Factors for One-Sided Tolerance Limits and for Variable Sampling Plans, "SCR-607, March (1963).
18. Final Safety Analysis Report for YongGwang Units 3 and 4, KEPCO (1994).
19. B.S. Pei, et al., Evaluation of Performance of Five Correlations for PWR Applications, Proc. of the Int. Nuclear Power Plant Thermal Hydraulics and Operations Topical Mtg.,Taipei, Taiwan, R.O.C., Oct.(1984).
20. Y.S. Chen, et al., The Modifications of the EPRI-1 Correlation for PWR Applications, Transactions of the American Nuclear Society, 1984 Winter Meeting (1984).
21. M. E. Nissley, "Consideration for Comparing CHF correlations," 2nd International Topical Mtg. on NPP Thermal Hydraulics and Operations, Tokyo, Japan (1986).